24

Photo-Induced Carrier Density, Optical Conductance and Transmittance in Graphene in the Presence of Optic-Phonon Scattering

W. Xu and H.M. Dong
Department of Physics, Yunnan University & Key Laboratory of Materials Physics, Institute of Solid State Physics, Chinese Academy of Sciences
P. R. China

1. Introduction

Since the experimental discovery of graphene in 2004 (Novoselov et al., 2004), the investigation of graphene-based electronics and optoelectronics has quickly become one of the most important research topics in condensed matter physics, nano-material science and nano-electronics (Zhang et al., 2005; Berger et al., 2006). Due to its excellent electronic transport, optical, and optoelectronic properties, such as high carrier density (up to 10^{13} cm^{-2}) and high carrier mobility at room temperature (up to 20 m^2/Vs) along with the high optical transmittance in the air-graphene-wafer systems, graphene has been proposed as an advanced material for new generation of electronic and optoelectronic devices. Graphene-based electronic devices exhibit high carrier mobility and quasi ballistic transport over sub-micron scales even at room temperature (Novoselov et al., 2005). It has already been used to realize high-speed and high-frequency electronic devices such as field-effect transistors (Castro et al., 2007), p-n junctions (González & Perfetto, 2008), high-frequency devices (Lin et al., 2009), to mention but a few. Very recently, graphene has also been proposed as an advanced transparent conducting material by utilizing its combined excellent transport and optical properties (Eda et al., 2008). It has been shown that graphene can be used to replace conventional indium tin oxide (ITO) transparent electrodes for making better and cheaper optical displays such the LCDs and LEDs (Hogan, 2008). Presently, graphene-based transparent electronics is a hot field of research for both fundamental studies and device applications (Eda et al., 2008).

For the usage of graphene as optoelectronic and transparent electronic devices, the investigation of its optical and optoelectronic properties is critical and essential. Recent experimental and theoretical work has demonstrated and predicted some particular and interesting optoelectronic properties in the infrared-to-visible spectral range for air-graphene-wafer systems. In particular, the results obtained from optical transmission (Kuzmenko et al., 2008) and infrared absorption (Li et al., 2008) measurements show the following features. (i) The optical conductance per graphene layer is a universal value $\sigma_0 = e^2/(4\hbar)$ in the visible frequency range (Kuzmenko et al., 2008; Li et al., 2008), which can be viewed as an intrinsic property of two-dimensional massless fermions. (ii) The corresponding light transmittance of monolayer and bilayer graphene on SiO_2 or Si wafers are, respectively,

about 0.98 and 0.96 in the visible bandwidth (Li et al., 2008; Nair et al., 2008). (iii) There is an optical absorption window (Kuzmenko et al., 2008; Li et al., 2008; Choi et al., 2009) for radiation photon energy smaller than 0.2 eV. The width and depth of this window depend strongly on the temperature (Kuzmenko et al., 2008) and carrier density (or gate voltage) in graphene samples (Li et al., 2008). This interesting finding implies that graphene can also be used for infrared detection in ambient conditions. Further experimental investigation shows that graphene can have strong intra- and inter-band transitions which can be substantially modified through electrical gating, similar to the resistance tuning in graphene field-effect transistors (Li et al., 2008; Wang et al., 2008). The optical and optoelectronic properties of graphene-based electronic systems have also been studied theoretically (Vasko & Ryzhii, 2008; Falkovsky & Pershoguba, 2007; Satuber et al., 2008). Most of the theoretical results are in line with the main experimental findings but are valid for low temperatures and only electron scattering by acoustic phonons was considered (Vasko & Ryzhii, 2008). However, most of the experimental studies of the optical properties of graphene systems have been undertaken at relatively high temperatures and up to room temperature (Kuzmenko et al., 2008; Li et al., 2008). In particular, the published theoretical work has not yet given a fully satisfactory explanation of the optical absorption window, present in graphene in the infrared bandwidth, that is observed experimentally by different kinds of measurements (Kuzmenko et al., 2008; Li et al., 2008; Choi et al., 2009). Therefore, in this study we examine how carriers in graphene respond to the applied radiation field in order to have a better understanding of the optoelectronic features of graphene, especially in the infrared wavelength regime. Here we would like to point out that graphene is a gapless electronic system in which optical phonon energy is about 196 meV (Ando, 2007). Hence, in contrast to a conventional semiconductor materials which normally have a band-gap much lager than the phonon energy, phonon scattering is expected to play an important role in affecting the electronic transitions accompanied by the emission and absorption of photons in graphene, especially in the infrared bandwidth. For the gapless graphene, the electrons in the valence band can gain the energy from the radiation field via optical absorption and be excited into the conduction band, while the electrons in the conduction band can lose energy via emission of phonons and be relaxed into the valence band. Together with the fact that the electrons interact more strongly with phonons than with photons, carrier-phonon interaction is an important factor in affecting the inter-band electronic transitions and, therefore, in determining the optoelectronic properties of graphene at relatively high-temperatures. In this work we develop a systematic approach to calculate the electronic and optical coefficients of graphene in the presence of a radiation field. In such an approach, the electron-photon and electron-phonon couplings are included in the calculation and their consequences are examined in a consistently theoretical manner.

2. Theoretical approach

2.1 Electronic transition rate

We consider a configuration where the graphene sheet is placed on the (x, y) plane on top of a dielectric wafer such as SiO_2/Si substrate. A light field is applied perpendicular to the graphene layer and is polarized linearly along the x direction of the system. In the effective-mass approximation, a carrier (electron or hole) in a monolayer graphene can be described by Weyl's equation for a massless neutrino (McCann & Falko, 2006). The single-particle Hamiltonian that describes a Dirac quasi-particle in the π bands near the K point can be obtained from, e.g., the usual $\mathbf{k} \cdot \mathbf{p}$ approach. We assume that the system under

study can be separated into the carriers of interest and the rest of the graphene crystal. Then the Hamiltonian that describes a carrier-photon-phonon system in graphene is:

$$H(t) = H_0 + H_{co}(t) + H_{ph} + H_{cp}(t). \tag{1}$$

Here,

$$H_0 = \gamma \begin{bmatrix} 0 & \vec{k}_x - i\vec{k}_y \\ \vec{k}_x + i\vec{k}_y & 0 \end{bmatrix} \tag{2}$$

is the Hamiltonian for a Dirac quasi-particle and $\gamma = \hbar v_F$ is the band parameter with $v_F = 10^8$ cm/s being the Fermi velocity for a carrier in graphene, and $\vec{k}_x = -i\partial/\partial x$ is the momentum operator along the x direction. The Schrödinger equation regarding H_0 can be solved analytically. The corresponding eigenvalue and eigenfunction are respectively

$$E_\lambda(\mathbf{k}) = \lambda\gamma|\mathbf{k}| = \lambda\gamma k \tag{3}$$

and

$$\psi_{\lambda\mathbf{k}}(\mathbf{r}) = |\mathbf{k}, \lambda >= 2^{-1/2}[1, \lambda e^{i\phi}]e^{i\mathbf{k}\cdot\mathbf{r}} \tag{4}$$

in the form of a row matrix. Here, $\mathbf{k} = (k_x, k_y)$ is the wavevector for a carrier, $k = \sqrt{k_x^2 + k_y^2}$, $\mathbf{r} = (x, y)$, $\lambda = +1$ for an electron and $\lambda = -1$ for a hole, and ϕ is the angle between $\mathbf{k}$ and the x direction. Using the usual coulomb gauge, the radiation field can be included by taking $k_x \to k_x - eA(t)/\hbar$ in Eq. (2) with $A(t)$ being the vector potential of the radiation field which is polarized along the x-direction. Thus, we can obtain the carrier-photon interaction Hamiltonian, which reads

$$H_{co}(t) = \frac{\gamma e A(t)}{\hbar} \begin{bmatrix} 0 & 1 \\ 1 & 0 \end{bmatrix}, \tag{5}$$

where $A(t) = (F_0/\omega)\sin(\omega t)$ with F_0 and ω being, respectively, the electric field strength and frequency of the radiation field. Furthermore, H_{ph} is the phonon Hamiltonian and

$$H_{cp}(t) = V_{\mathbf{q}} a_{\mathbf{q}} e^{i(\mathbf{q}\cdot\mathbf{r} - \omega_q t)} + V_{\mathbf{q}}^* a_{\mathbf{q}}^\dagger e^{-i(\mathbf{q}\cdot\mathbf{r} + \omega_q t)} \tag{6}$$

describes carrier interaction with 2D-like phonons, where $\mathbf{q} = (q_x, q_y)$ is the phonon wave vector in the (x, y) plane, $(a_{\mathbf{q}}^\dagger, a_{\mathbf{q}})$ are the canonical conjugate coordinates of the phonon system, $V_{\mathbf{q}}$ is the carrier-phonon interaction coefficient, and ω_q is the phonon frequency in graphene. For the case of a relatively weak radiation field and weak carrier-phonon interaction, $H_{co}(t)$ and $H_{cp}(t)$ can be treated as perturbations. Using Fermi's golden rule (Stroscio & Mitra, 2005), the first-order steady-state electronic transition rate is given by

$$W_{\lambda\lambda'}(\mathbf{k}, \mathbf{k}') = \sum_\nu W_{\lambda\lambda'}^\nu(\mathbf{k}, \mathbf{k}'); \tag{7}$$

it is the probability for scattering of a carrier from a state $|\mathbf{k}, \lambda >$ to a state $|\mathbf{k}', \lambda' >$ due to interaction with photons and phonons. Moreover, ν refers to different scattering mechanisms. In Eq. (7) the rate

$$W_{\lambda\lambda'}^{co_\nu\pm}(\mathbf{k}, \mathbf{k}') = \frac{2\pi}{\hbar}\left(\frac{eF_0\gamma}{2\hbar\omega}\right)^2 \frac{1 + \lambda\lambda'\cos(2\phi)}{2}\delta_{\mathbf{k}',\mathbf{k}}\delta[E_\lambda(\mathbf{k}) - E_{\lambda'}(\mathbf{k}') \pm \hbar\omega]$$

is induced by direct carrier-photon interaction via absorption (+ sign) and emission (− sign) of a photon with an energy $\hbar\omega$, and ϕ is the angle between $\mathbf{k}$ and the x axis. The rate

$$W^{cp,\pm}_{\lambda\lambda'}(\mathbf{k},\mathbf{k}') = \frac{2\pi}{\hbar}\begin{bmatrix} N_q \\ N_q+1 \end{bmatrix} |U^{cp}_{\lambda\lambda'}(\mathbf{q},\theta)|^2 \delta_{\mathbf{k}',\mathbf{k}+\mathbf{q}} \delta[E_\lambda(\mathbf{k}) - E_{\lambda'}(\mathbf{k}') \pm \hbar\omega_q]$$

is induced by carrier-phonon interaction, where $N_q = (e^{\hbar\omega_q/k_BT}-1)^{-1}$ is the phonon occupation number, $|U^{cp}_{\lambda\lambda'}(\mathbf{q},\theta)|^2 = |<\mathbf{k}',\lambda'|V_\mathbf{q}|\mathbf{k},\lambda>|^2$, θ is the angle between $\mathbf{k}'$ and $\mathbf{k}$, and the terms N_q and N_q+1 correspond to the absorption and emission of a phonon, respectively. The rate

$$W^{cop}_{\lambda\lambda'}(\mathbf{k},\mathbf{k}') = \frac{4\pi}{\hbar}\begin{bmatrix} \sqrt{N_q} \\ \sqrt{N_q+1} \end{bmatrix} \frac{eF_0\gamma}{2\hbar\omega} \sum_{\mathbf{k}_1,\lambda_1} |U^{cp}_{\lambda_1\lambda'}(\mathbf{q},\theta)|^2 \sqrt{[1+\lambda\lambda_1\cos(2\phi)]/2}$$

$$\times \delta_{\mathbf{k},\mathbf{k}_1}\delta_{\mathbf{k}',\mathbf{k}_1+\mathbf{q}}\delta[E_\lambda(\mathbf{k}) - E_{\lambda_1}(\mathbf{k}_1) \pm \hbar\omega + E_{\lambda_1}(\mathbf{k}_1) - E_{\lambda'}(\mathbf{k}') \pm \hbar\omega_q]$$

describes the coupled carrier-photon-phonon scattering via absorption and emission of both photons and phonons. This term also represents the indirect optical and electronic transition channels.

Here we consider only carrier interaction with optical phonons. It is known that at relatively high-temperatures carriers in graphene interact more strongly with optical phonons (Xu et al., 2009). This coupling can result in a relatively large energy relaxation due to the inelastic nature of the scattering. Moreover, the published experimental results (Kuzmenko et al., 2008; Li et al., 2008; Choi et al., 2009) show that the optical absorption window in graphene occurs near the photon energy regime $\hbar\omega \sim 0.1$ eV. This energy is much larger than the acoustic phonon energy in graphene. As a result, at relatively high-temperatures we can neglect the effect of the quasi-elastic scattering by acoustic phonons. On the basis of the valence-force-field model, the coupling coefficient for carrier interaction with long-wavelength optical phonons in graphene is (Ando, 2007; Tse & Sarma, 2007)

$$V^\mu_\mathbf{q} = -g\gamma M^\mu_\mathbf{q}. \tag{8}$$

Here $g = (\hbar\mathcal{B}/b^2)/\sqrt{2\rho\hbar\omega_0}$, $\rho \simeq 6.5\times10^{-8}$ g/cm^2 is the areal density of the graphene sheet, $\omega_0 = 196$ meV the optical phonon frequency at the Γ-point, $\mathcal{B} = -d(\ln\gamma_0)/d(\ln b) \sim 2$ is a dimensionless parameter that relates to the change of the resonance integral γ_0 between nearest neighbor carbon atoms (Ando, 2007), and $b = a/\sqrt{3}$ is the equilibrium bond length. Furthermore,

$$M^l_\mathbf{q} = \begin{bmatrix} 0 & -e^{-i\phi_q} \\ e^{i\phi_q} & 0 \end{bmatrix} \text{ and } M^t_\mathbf{q} = \begin{bmatrix} 0 & ie^{-i\phi_q} \\ ie^{i\phi_q} & 0 \end{bmatrix}, \tag{9}$$

describe the coupling with, respectively, longitudinal (l) and transverse (t) phonon modes, and ϕ_q is the angle between $\mathbf{q}$ and the x axis. The carrier-phonon scattering matrix elements are

$$|U^l_{\lambda\lambda'}(\mathbf{q},\mathbf{k})| = (g\gamma/\sqrt{2})[1-\lambda'\lambda\cos(\phi+\phi'-2\phi_q)]^{1/2}$$

and

$$|U^t_{\lambda\lambda'}(\mathbf{q},\mathbf{k})| = (g\gamma/\sqrt{2})[1+\lambda'\lambda\cos(\phi+\phi'-2\phi_q)]^{1/2}.$$

2.2 Balance equations

In this research work we employ the semi-classical Boltzmann equation (BE) to study the response of the carriers in graphene to an applied radiation field. It is known that the Boltzmann equation is a powerful tool to study theoretically the linear and nonlinear responses of electrons in an electron gas system under the action of external driving ac and dc fields. In contrast to the Kubo formula based quantum theory which handles essentially the linear response, the BE can be used to study nonlinear transport and optical effects (Xu et al., 1991). In particular, the balance equation approach based on the BE can be used to study non-equilibrium electronic transport and to calculate corresponding coefficients self-consistently such as the electron density and electron drift velocity in different states (Xu, 2005). Hence, we would like to use a consistent and tractable theory to calculate both photo-excited carrier density and photo-induced electron energy loss in graphene. The BE based balance equation approach is therefore a good theoretical option. It should be noted that although the momentum- and energy-balance equations proposed by Lei and Ting (Lei, 1998) based on quantum approach can handle the nonlinear transport of electrons under strong dc and/or intense ac fields, they can only be used to calculate the averaged electron drift velocity and electron energy loss rate. This approach cannot be applied to evaluate the electron density in different states. Furthermore, by employing the balance equation approach on the basis of the BE to study graphene (Xu et al., 2009; Dong et al., 2008), we have already achieved a good agreement between theoretical results and experimental findings both qualitatively and quantitatively. The Boltzmann transport theory has also been applied to investigate graphenen system by other authors (Vasko & Ryzhii, 2008). It was found (Vasko & Ryzhii, 2008) that for a homogeneous graphene system with relatively high carrier density and long mean free path (which is indeed the case for graphene), such a theory can lead to the same results as those obtained from quantum transport theory (Falkovsky & Pershoguba, 2007; Satuber et al., 2008). For non-degenerate statistics, the BE can be written as

$$\frac{\partial f_\lambda(\mathbf{k})}{\partial t} = g_s g_v \sum_{\lambda',\mathbf{k}',\nu} [F^\nu_{\lambda'\lambda}(\mathbf{k}',\mathbf{k}) - F^\nu_{\lambda\lambda'}(\mathbf{k},\mathbf{k}')], \tag{10}$$

where $g_s = 2$ and $g_v = 2$ account, respectively, for spin and valley degeneracy, $f_\lambda(\mathbf{k})$ is the momentum distribution function for a carrier in a state $|\mathbf{k},\lambda>$, and $F^\nu_{\lambda'\lambda}(\mathbf{k}',\mathbf{k}) = f_{\lambda'}(\mathbf{k}')[1-f_\lambda(\mathbf{k})]W^\nu_{\lambda'\lambda}(\mathbf{k}',\mathbf{k})$. Because the radiation field has been included in the electronic transition rate, the force term induced by this field does not appear in the drift term on the left-hand side of the BE to avoid double-counting. There is no simple and analytical solution to Eq. (10) with $W_{\lambda'\lambda}(\mathbf{k}',\mathbf{k})$ given by Eq. (7). In the present study we employ the usual balance-equation approach to solve the problem. For the first moment, the mass-balance equation (or rate equation) can be derived after operating with $g_s g_v \sum_{\mathbf{k}}$ on both sides of the BE. The obtained result is

$$\frac{\partial n_e}{\partial t} = \frac{\partial n_h}{\partial t} = \frac{n_h}{\tau^\nu_{-+}} - \frac{n_e}{\tau^\nu_{+-}}, \tag{11}$$

where $1/\tau^\nu_{\lambda'\lambda} = (16/n_{\lambda'})\sum_\nu F^\nu_{\lambda'\lambda}$ is the rate for scattering of a carrier from band λ' to band λ due to the ν^{th} scattering center, $F^\nu_{\lambda'\lambda} = \sum_{\mathbf{k}',\mathbf{k}} F^\nu_{\lambda'\lambda}(\mathbf{k}',\mathbf{k})$, and n_e and n_h are, respectively, the electron and hole densities in different bands. This equation implies that only inter-band scattering (i.e., $\lambda' \neq \lambda$) can alter the number of carries in a band of the graphene system. It also reflects the fact that the change of the electron number in the conduction band equals that of the hole number in the valence band, namely this equation expresses the charge number conservation in the system.

For the second moment, the energy-balance equation can be derived by operating with $\sum_{\mathbf{k},\lambda} E_\lambda(\mathbf{k})$ on both sides of the BE. From the energy-balance equation we obtain the energy transfer rate for a carrier, $P_\lambda = \sum_{\mathbf{k}} E_\lambda(\mathbf{k})\partial f_\lambda(\mathbf{k})/\partial t$, and the total energy transfer rate of the system is $P = P_+ + P_- = P_{ph} - P_{op}$, where

$$P_{op} = 4\hbar\omega \sum_{\lambda',\lambda} (F^{co,+}_{\lambda\lambda'} - F^{co,-}_{\lambda\lambda'} + F^{cop}_{\lambda\lambda'}) \tag{12}$$

is the energy transfer rate induced by optical absorption and emission via direct and indirect transition channels, and $F^{co,\pm}_{\lambda\lambda'}$ describes the absorption (+) and emission (-) of photons. Further,

$$P_{ph} = \pm 4 \sum_{\lambda',\lambda} \hbar\omega_q (F^{cp,\pm}_{\lambda\lambda'} + F^{cop}_{\lambda\lambda'}) \tag{13}$$

is the energy transfer rate induced by emission or absorption of optical phonons. In the steady state, $P = 0$ and $P_{op} = P_{ph}$ gives an energy conservation law, namely the carriers in the system gain energy from the radiation field via absorption of photons and phonons and lose energy via emission of optical phonons and photons.
For coupled carrier-photon-phonon scattering via absorption and emission of photons and optical phonons, we have

$$W^{cop}_{\lambda\lambda'}(\mathbf{k},\mathbf{k}') = \frac{4\pi}{\hbar}\left[\frac{\sqrt{N_0}}{\sqrt{N_0+1}}\right]\frac{eF_0 g\gamma^2}{2\hbar\omega}(\cos\Phi + \sin\Phi)(\cos\phi + \sin\phi)$$

$$\times\delta_{\mathbf{k}',\mathbf{k}+\mathbf{q}}\delta[E_\lambda(\mathbf{k}) - E_{\lambda'}(\mathbf{k}') + \hbar\omega \pm \hbar\omega_q],$$

with $\Phi = (\phi + \phi' - 2\phi_q)/2$. As a result, we explicitly obtain

$$F^{cop}_{+-} = F^{cop}_{-+} = 0. \tag{14}$$

This result implies that in graphene the coupled carrier-photon-phonon interaction via coupling with long wavelength optical phonons does not contribute to electronic transitions. In the steady state, i.e., for $dn_e/dt = dn_h/dt = 0$, the mass-balance equation becomes

$$F^{co,+}_{-+} + F^{cp,-}_{-+} = F^{cp,+}_{+-} + F^{co,-}_{+-}, \tag{15}$$

which reflects the fact that electrons pumped from the valence band into the conduction band are balanced by those relaxed from the conduction band into the valence band. Furthermore, the energy transfer rate induced by optical absorption in the steady state is

$$P_{op} = 4\hbar\omega \sum_{\lambda',\lambda} [F^{co,+}_{\lambda\lambda'} - F^{co,-}_{\lambda\lambda'}]. \tag{16}$$

When a graphene sheet is subjected to a radiation field, electrons in the occupied states, e.g., in the lower energy $\lambda = -$ band, are excited into the empty states, e.g., of the higher energy $\lambda = +$ band, so that an optical absorption occurs.
One of the advantages of the balance-equation approach is that we can avoid the difficulties to solve the BE directly and instead use a certain form of the carrier distribution function to calculate the physical quantities. Here we use the Fermi-Dirac type of statistical energy distribution as approximately the momentum distribution for a carrier, i.e., $f_\lambda(\mathbf{k}) \simeq f_\lambda(\lambda\gamma k)$, with $f_\lambda(x) = [1 + e^{(x-\mu^*_\lambda)/k_BT}]^{-1}$ where μ^*_λ is the quasi Fermi energy (or quasi chemical potential) for electrons or holes in the presence of the radiation field. For carrier-photon

interaction via inter- and intra-band transition channels we have $F_{+-}^{co,+} = F_{-+}^{co,-} = F_{++}^{co,-} = F_{--}^{co,-} = 0$,

$$F_{-+}^{co,+} = \frac{e^2F_0^2}{32\hbar^2\omega} f_-(-\frac{\hbar\omega}{2})[1 - f_+(\frac{\hbar\omega}{2})] \tag{17}$$

is for optical absorption from the valence band to the conduction band,

$$F_{+-}^{co,-} = \frac{e^2F_0^2}{32\hbar^2\omega} f_+(\frac{\hbar\omega}{2})[1 - f_-(-\frac{\hbar\omega}{2})] \tag{18}$$

is for optical emission from the conduction band to the valence band, and

$$F_{\lambda\lambda}^{co,+} = \frac{e^2F_0^2}{8\pi\hbar^4\omega^3} \frac{\omega\tau_\lambda}{1 + (\omega\tau_\lambda)^2} \int_0^\infty dEEf_\lambda(\lambda E)[1 - f_\lambda(\lambda E)] \tag{19}$$

is induced by intra-band optical absorption in the conduction band ($\lambda = 1$) and valence band ($\lambda = -1$) with τ_λ being the energy relaxation time for an electron or a hole in different bands. In fact, this term is caused by the usual free-carrier absorption channels. The energy relaxation time is used to describe the broadening of the scattering states, which can result in a spectrum structure for the intra-band optical absorption. It should be noted that for intra-band free-carrier absorption, the momentum conservation law still holds (i.e., for optical transitions the electron momentum at initial and final states must be the same during a scattering event, as given by Eq. (4)). However, in the presence of the external driving fields such as the radiation fields and of the scattering centers such as impurities and phonons, the scattering states are damped and broadened. As a result, the δ-function in Eq. (7) for intra-band optical transition can be replaced through Poisson Kernel: $\delta(E) \to (E_\lambda/\pi)(E^2 + E_\lambda^2)^{-1}$ with $E_\lambda = \hbar/\tau_\lambda$ being the energy broadening of the states.

For carrier-phonon interaction via different transition channels, we have $F_{+-}^{cp,-} = F_{-+}^{cp,+} = 0$,

$$F_{+-}^{cp,+} = \frac{g^2(N_0 + 1)}{2\pi\hbar\gamma^2} \int_0^{\hbar\omega_0} dxx(\hbar\omega_0 - x)f_+(x)[1 - f_-(x - \hbar\omega_0)] \tag{20}$$

is for phonon emission and corresponding electronic transition from the conduction band to the valence band, with $N_0 = [e^{\hbar\omega_0/k_BT} - 1]^{-1}$ and $\omega_q \to \omega_0$ a constant at the Γ-point for long-wavelength optical phonons, and

$$F_{-+}^{cp,-} = \frac{g^2N_0}{2\pi\hbar\gamma^2} \int_0^{\hbar\omega_0} dxx(\hbar\omega_0 - x)f_-(-x)[1 - f_+(\hbar\omega_0 - x)], \tag{21}$$

is induced by the absorption of phonons and corresponding electronic transition from the valence band to the conduction band.

2.3 Photo-induced carriers

We now consider a graphene layer in which the conducting carriers are electrons (or a positive gate voltage is applied) in the absence of the radiation field (or in the dark). When a light field is applied to the system, the electrons in the valence band are excited into the conduction band so that photo-excited carriers can be induced. If n_0 is the electron density in the absence of the radiation field (or dark density) at $F_0 = 0$, the electron density at $F_0 \neq 0$ is $n_e = n_0 + \Delta n_e$. On

account of charge number conservation we have $\Delta n_e = n_h$, the hole density in the presence of radiation field. Thus, we get

$$n_e = n_0 + n_h, \tag{22}$$

with

$$n_e = g_s g_v \sum_{\mathbf{k}} f_+(\mathbf{k}) = \frac{2}{\pi\gamma^2} \int_0^\infty \frac{dx\ x}{e^{(x-\mu_e^*)/k_BT}+1} \tag{23}$$

and

$$n_h = n_e - n_0 = g_s g_v \sum_{\mathbf{k}} [1 - f_-(\mathbf{k})] = \frac{2}{\pi\gamma^2} \int_0^\infty \frac{dx\ x}{e^{(x+\mu_h^*)/k_BT}+1}. \tag{24}$$

With the mass-balance equation given by Eq. (15) and the requirement of the charge number conservation shown as Eq. (22) we can determine the quasi chemical potentials μ_λ^* for electrons and holes. Then the electron density n_e and hole density n_h can be obtained in the presence of the radiation field F_0. We notice that this approach can also be applied to p-type graphene samples, when a negative gate voltage is applied so that the conducting carriers are holes in the valence band in the dark.

2.4 Optical conductance and transmission

With the obtained carrier chemical potential μ_λ^* we can calculate $F_{\lambda\lambda'}^{co,\pm}$. From the carrier energy transfer rate induced by optical absorption, described by Eq. (16), we can calculate the optical conductance $\sigma(\omega)$ for graphene using the expression (Wei et al., 2007)

$$\sigma(\omega) = 2P_{op}/F_0^2 = 8\hbar\omega \sum_{\lambda,\lambda'} (F_{\lambda,\lambda'}^{co,+} - F_{\lambda,\lambda'}^{co,-})/F_0^2. \tag{25}$$

Moreover, the transmission coefficient for a device with a graphene layer on top of a substrate, namely for an air-graphene-wafer system, is given by (Satuber et al., 2008)

$$T(\omega) = \sqrt{\frac{\epsilon_2}{\epsilon_1}} \frac{4(\epsilon_1\epsilon_0)^2}{|(\sqrt{\epsilon_1\epsilon_2}+\epsilon_1)\epsilon_0 + \sqrt{\epsilon_1}\sigma(\omega)/c|^2}, \tag{26}$$

where $\epsilon_1 \simeq 1$ for air, ϵ_2 is the effective high-frequency dielectric constant of the substrate, and ϵ_0 and c are, respectively, the dielectric constant and the speed of light in vacuum. It indicates that the light transmittance of the graphene layer in an air-graphene-substrate system depends on the dielectric constant of the substrate material. Moreover, a substrate with a larger dielectric constant can result in a smaller light transmittance for the graphene layer.

3. Numerical results and discussions

In the numerical calculations we consider a typical air-graphene-SiO_2/wafer system. Thus, $\epsilon_1 \simeq \epsilon_0 = 1$ and $\epsilon_2 \simeq 2.0$. The effect of the dielectric mismatch between the graphene layer and the SiO_2 substrate has been taken into account using the image charge method (Dong et al., 2008). Furthermore, it has been obtained experimentally (Sun et al., 2008) that in graphene the energy relaxation time is about $\tau_\lambda \sim 1$ ps for high-density samples. Thus, we take $\tau_\lambda \sim 1$ ps in the calculation for free-carrier absorption. A typical electric field strength of the radiation field $F_0 = 500$ V/cm is used in most of the calculations.

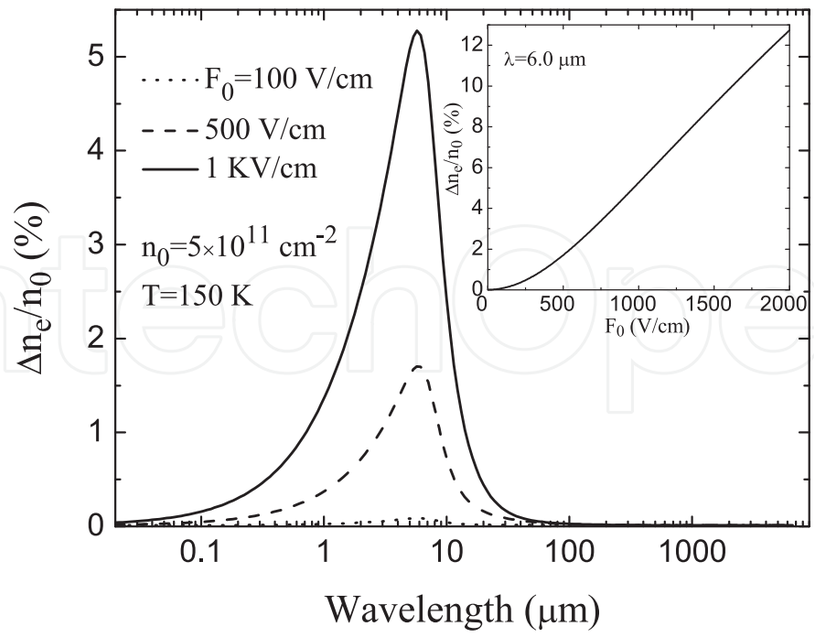

Fig. 1. Photo-excited electron density Δn_e as a function of the radiation wavelength, at temperature $T = 150$ K and a fixed dark electron density $n_0 = 5 \times 10^{11}$ cm^{-2}, for different strengths of the radiation field F_0. The inset shows Δn_e as a function of F_0 at a fixed radiation wavelength $\mathcal{L} = 6.0$ μm. Note that Δn_e is equal to n_h, the photo-induced hole density.

3.1 Photo-induced carrier densities

In Fig. 1 we show the dependence of the photon-excited electron density Δn_e on the radiation wavelength ($\mathcal{L}$) and radiation intensity for a fixed dark electron density n_0 and a temperature $T = 150$ K. Δn_e vs the strength of the radiation field F_0 is also shown in the inset for fixed radiation wavelength $\mathcal{L} = 6.0$ μm. It should be noted that $\Delta n_e = n_h$ is also the photo-induced hole density for a n-type graphene in the dark. As expected, the photo-induced carrier densities increase with radiation intensity $I \sim F_0^2$. For a typical radiation intensity with F_0 about 500 V/cm, several percents of photo-induced electron density can be achieved in graphene, similar to photo-excited carriers in conventional semiconductors. We notice that when the radiation wavelength is about $\mathcal{L} \sim 6$ μm Δn_e is maximum. Because the optical phonon wavelength in graphene is about 6 μm, the peak of Δn_e appears at about this wavelength. For $\mathcal{L} > 6$ μm, Δn_e decreases sharply with increasing $\mathcal{L}$. These results indicate that in graphene the photo-induced carrier densities can be observed clearly in the infrared bandwidth.

In Fig. 2 we show the photo-excited electron density Δn_e as a function of the radiation wavelength, at fixed dark electron density and radiation intensity, for different temperatures. We see that the photo-excited carrier densities are very sensitive to temperature. Δn_e decreases quickly with increasing temperature. Such a feature is typical when scattering by optical phonons is present. With increasing temperature, the phonon occupation number $N_0 = [e^{\hbar\omega_0/k_BT} - 1]^{-1}$ increases sharply so that a stronger phonon scattering occurs. The strong phonon scattering can bring electrons from the conduction band to the valence band via phonon emission. As a consequence, at relatively high temperatures less photo-excited electrons remain in the conduction band. Accordingly, Δn_e decreases with increasing

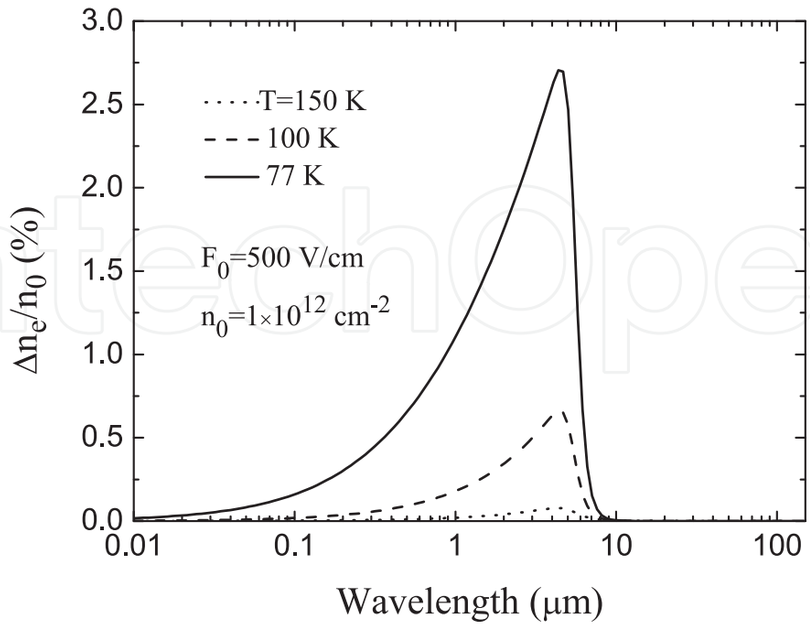

Fig. 2. Photo-excited electron density Δn_e as a function of the radiation wavelength, for fixed dark electron density $n_0 = 1 \times 10^{12}$ cm^{-2} and radiation intensity $F_0 = 500$ V/cm, at different temperatures.

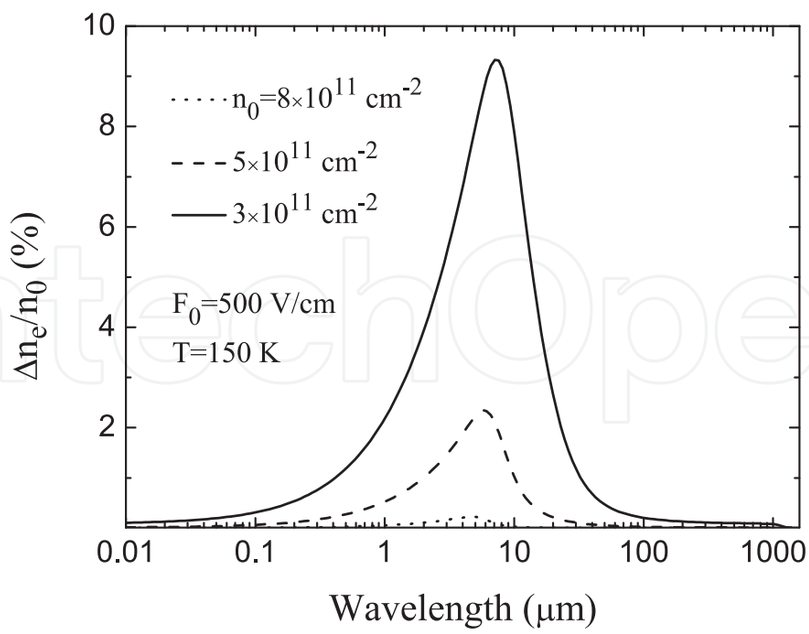

Fig. 3. Δn_e as a function of the radiation wavelength at a temperature $T = 150$ K and fixed strength of the radiation field $F_0 = 500$ V/cm, for different dark electron densities.

temperature. These results suggest that phonon scattering is an important mechanism in affecting the photo-excited carrier densities in graphene.

In Fig. 3 Δn_e is plotted as a function of the radiation wavelength, for $T = 150$ K and $F_0 = 500$ V/cm, for different dark electron densities. The main feature in Fig. 3 is that the photo-induced carrier density ratio $\Delta n_e/n_0$ decreases with increasing dark electron density n_0. At relatively weak levels of light excitation Δn_e changes only by several percents (see also Figs. 1 and 2). This implies that the change of the quasi Fermi levels in the system due to a weak excitation is not very significant. A larger n_0 means a higher Fermi level in the conduction band in the absence of the radiation field. As we know, the electrons make transitions mainly from the occupied states to the empty states in an electron gas system. For larger n_0 only the higher energy states above the Fermi level are available for photo-induced electrons to be excited to. Thus, larger photon energy (or shorter wavelength radiation) is required to excite electrons from the valence band to the conduction band. On the other hand, because of the linear energy spectrum for carriers in graphene, larger energy states correspond to larger momentum states in the conduction band. Since the electron-phonon scattering alters both the energy and momentum, as required by the corresponding energy and momentum conservation laws, larger momentum states can result in stronger electron-phonon coupling. Again, the strong phonon scattering can reduce the photo-induced electron density in the conduction band. Therefore, the densities shown in Fig. 3 are, at least partly, the result of electron-phonon interaction. Moreover, it should be noted that the dark carrier density in graphene can be modulated effectively by applying a gate voltage (Li et al., 2008; Wang et al., 2008). Hence, the densities of photo-induced carriers can be modulated electrically as well.

The main results from Figs. 1 - 3 are as follows. (i) The photo-induced electron density increases with radiation wavelength for $\mathcal{L} < 6.0$ μm. (ii) The peak of the photo-excited electron density can be observed around $\mathcal{L} \sim 6.0$ μm, which corresponds to the optical phonon energy $\hbar\omega_0 = 196$ meV in graphene. (iii) The photo-induced electron density decreases rapidly with increasing radiation wavelength for $\mathcal{L} > 6.0$ μm. When a graphene sample is subjected to a radiation field and the electron-phonon interaction is present, electrons in the valence band can gain energy from the radiation field through optical absorption and be excited into the conduction band, while electrons in the conduction band can lose energy via emission of phonons and be relaxed into the valence band. The balance of these two competing processes results in the photo-induced carriers in the system in the steady state. As we know, the optical phonon emission occurs when the electron energy is larger than the optical phonon energy (Xu et al., 1993). For $\mathcal{L} < 6.0$ μm electrons located around the top of the valence band can gain a photon energy $\hbar\omega > \hbar\omega_0$ via optical absorption and be excited into the conduction band. These electrons can lose energy $\hbar\omega_0$ through emission of optical phonons and be relaxed into the empty states of the valence band. This is why photo-excited carrier densities increase with the radiation wavelength for $\mathcal{L} < 6.0$ μm. At relatively long-wavelength radiations for $\mathcal{L} > 6.0$ μm, the electrons around the top of the valence band gain energy $\hbar\omega < \hbar\omega_0$ and are excited into the conduction band. However, when the electron energy is less than the optical phonon energy electronic transitions via phonon emission are much less likely (Xu et al., 1993). Thus, for $\hbar\omega < \hbar\omega_0$ the electrons in the conduction band are less likely to be relaxed into the valence band though electron-phonon coupling. This is the main reason why the photo-excited carrier densities decrease sharply with increasing radiation wavelength for $\hbar\omega < \hbar\omega_0$. When the photon energy is close to the optical phonon energy $\hbar\omega \sim \hbar\omega_0$, inter-band electronic transitions can occur through a process in which the electrons gain a photon energy $\hbar\omega$ from the radiation field and lose a phonon energy $\hbar\omega_0$ via phonon emission.

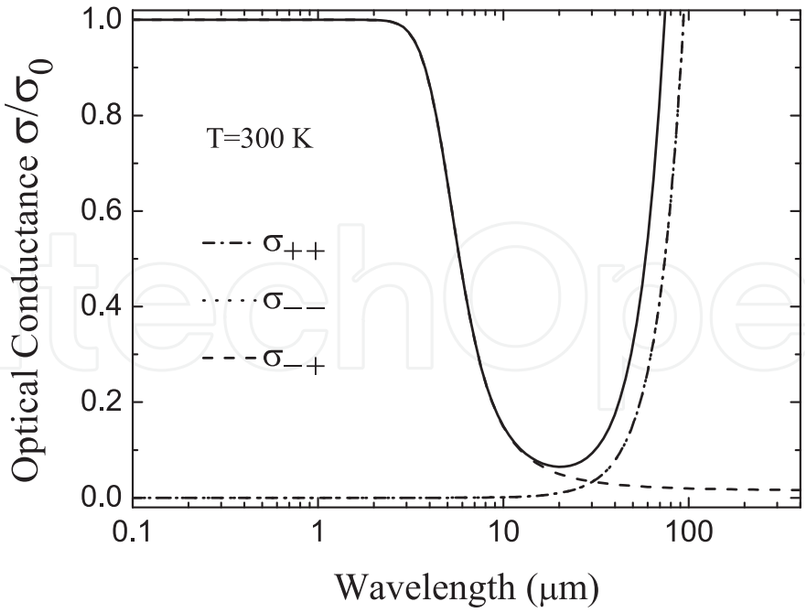

Fig. 4. Contribution to the total optical conductance (solid line) from different transition channels at room temperature for a fixed dark electron density $n_0 = 1 \times 10^{12}$ cm^{-2}. Here $\sigma_0 = e^2/(4\hbar)$ and σ_{-+} (dashed curve) is for transition from valence band $(-)$ to conduction band $(+)$. The curves for intra-band transitions, σ_{++} and σ_{--}, coincide roughly.

Thus, a resonant transition occurs in graphene. Such a mechanism is electrically equivalent to the electro-phonon resonance effect (Xu et al., 1993) proposed previously by us. As a result, the strongest inter-band electronic transitions can occur for $\hbar\omega \sim \hbar\omega_0$. That is, a peak of the photo-induced carrier density can be observed in graphene when the radiation frequency is close to the optical phonon frequency. The theoretical results discussed here indicate that in gapless graphene the scattering by optical phonons plays an important role in affecting photo-excited carrier densities.

3.2 Optical conductance and transmission

In Fig. 4, we show the contributions from different transition channels to the optical conductance $\sigma(\omega)$ or optical absorption for a fixed dark electron density n_0 at room temperature. We notice the following features. (i) Inter-band transitions contribute to the optical absorption in the short-wavelength regime ($\mathcal{L} < 3$ μm), whereas intra-band transitions give rise to the long-wavelength optical absorption. (ii) The optical absorption varies very little upon varying the radiation frequency in the short-wavelength regime ($\mathcal{L} < 3$ μm), whereas the optical conductance or absorption coefficient depends strongly on the radiation wavelength in the long-wavelength regime ($\mathcal{L} > 3$ μm). (iii) The optical conductance in the short-wavelength regime is a universal value $\sigma_0 = e^2/(4\hbar)$ in monolayer graphene as discovered experimentally (Kuzmenko et al., 2008; Li et al., 2008; Nair et al., 2008). (iv) More interestingly, there is an infrared absorption window in the $4 \sim 100$ μm wavelength range. As expected, inter-band transitions require larger photon energy. Intra-band transitions, which are caused by the usual free-carrier absorption, occur under low photon energy radiation. It is a common feature for free-carrier absorption that the strength of the optical absorption increases rapidly with radiation wavelength (Li, 2006). We find that the optical absorption window observed experimentally (Kuzmenko et al., 2008; Li et al., 2008; Choi et al., 2009) is

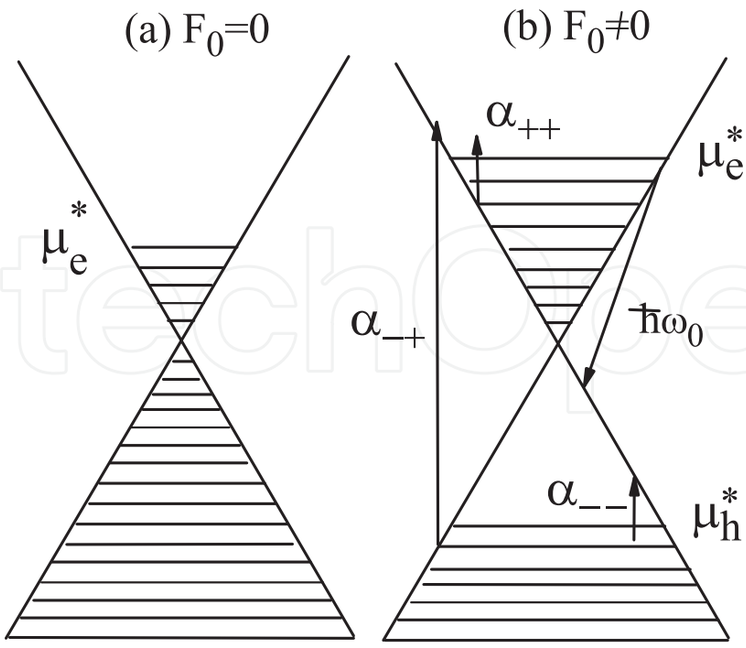

Fig. 5. (a) A graphene system in the absence of the radiation field ($F_0 = 0$). The conducting carriers are electrons with a Fermi energy μ_e^* in the conduction band. The hatched area shows the occupied states. (b) Optical absorption channels in the presence of a radiation field ($F_0 \neq 0$). Here μ_e^* and μ_h^* are the quasi Fermi energies for, respectively, electrons and holes and there are three optical absorption channels: α_{-+}, α_{++}, and α_{--}. $\hbar\omega_0$ is the energy of an emitted optical phonon.

induced by the competing absorption channels due to inter- and intra-band scattering events in graphene. This can explain and reproduce recent experimental findings (Kuzmenko et al., 2008; Li et al., 2008; Choi et al., 2009).

The interesting features of optical absorption in graphene can be understood with the help of Fig. 5. When the radiation field is absent, there is a single Fermi level (or chemical potential) in the conduction band in a n-type graphene sample (or in the presence of a positive gate voltage). In this case all states below μ_e^* are occupied by electrons as shown in Fig. 5 (a). When a radiation field is applied to the system (see Fig. 5 (b)), the electrons in the valence band can gain energy from the radiation field and be excited into the conduction band via absorption of photons. Thus, the electron density in the conduction band increases and so does the quasi Fermi level μ_e^* for electrons. Meanwhile, the holes are left in the valence band and a quasi Fermi level μ_h^* is established in this band for them. As shown in Fig. 5 (b), in the presence of a radiation field the intra-band electronic transition accompanied by the absorption of photons can occur not only in the conduction band via the α_{++} channel but also in the valence band via the α_{--} channel. The intra-band transitions are a direct consequence of the broadening of the scattering states in the conduction and valence bands. At the same time, the electrons in the conduction band can lose energy via emission of optical phonons and relax into the valence-band. The electrons in the valence band can also gain energy by absorption of optical phonons and be excited into the conduction band due to the inelastic character of the electron-phonon scattering, although such a process is much weaker than that for phonon emission. Because graphene is a gapless semiconductor, the electrons in the valence band can be more easily excited into the conduction band via optical absorption and

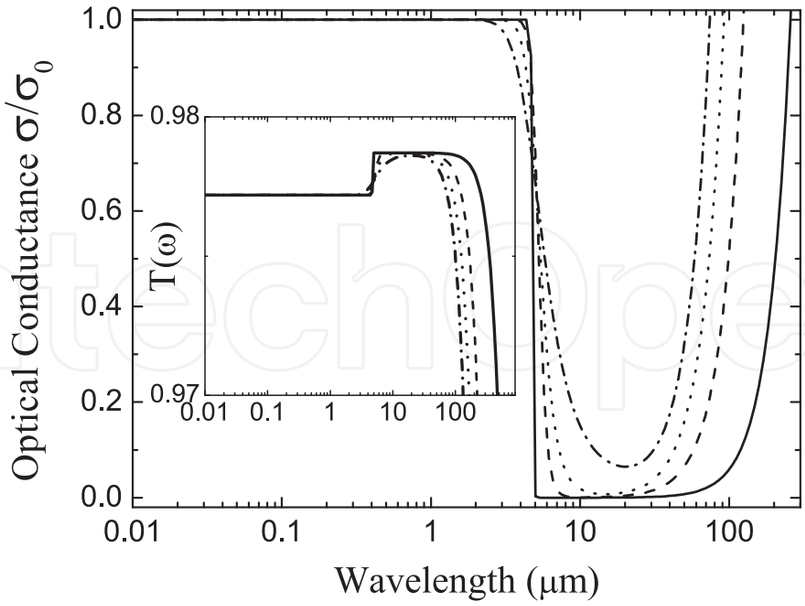

Fig. 6. Optical conductance and transmission coefficient (inset) as a function of the radiation wavelength, at a fixed dark electron density $n_0 = 1 \times 10^{12}$ cm^{-2}, for different temperatures $T = 10$ K (solid curve), 77 K (dashed curve), 150 K (dotted curve) and 300 K (dotted-dashed curve).

those in the conduction band can be easily relaxed into the valence band via phonon emission, in contrast to a conventional semiconductor. Thus, there is a strong inter-band optical and electronic transition channel (i.e., α_{-+} in Fig. 5 (b)) in graphene. Since optical absorption and phonon emission events describe transitions from occupied states to empty states, the intra-band transitions require less photon energy whereas a relatively larger photon energy is needed for inter-band transitions. Consequently, an optical absorption window can be induced through different energy requirements for inter- and intra-transition channels.

In Fig. 6 we show the optical conductance σ and transmission coefficient $T(\omega)$ as a function of the radiation wavelength, at fixed dark electron density n_0, for different temperatures. As can be seen, in the short-wavelength regime $\mathcal{L} < 3$ μm, both σ and $T(\omega)$ depend very little on the radiation wavelength. This confirms that σ does not depend on temperature under short-wavelength radiation in graphene. The corresponding transmission coefficient $T(\omega)$ is about $0.97 \sim 0.98$ in the short-wavelength regime and agrees quantitatively with the experimental data (Nair et al., 2008). In the long-wavelength regime, in which the optical absorption window can be observed, both the optical conductance and light transmittance depend sensitively on the temperature, which is in line with the experimental findings (Kuzmenko et al., 2008). It should be noted that for fixed electron and hole densities, the quasi chemical potential for electrons/holes decreases/increases with increasing temperature. Thus, due to the Pauli blockade effect (Krenner et al., 2006), a blue shift of the optical absorption window with decreasing temperature can be observed as shown in Fig. 6. We note that the strength of the optical absorption is proportional to the optical conductance. Therefore, the height of the optical absorption window decreases with increasing temperature. We find that a wider and deeper optical absorption window and a sharper cut-off of the optical absorption at the window edges can be observed at lower temperatures. These theoretical results can be used to explain the strong dependence of the optical conductance on temperature in the

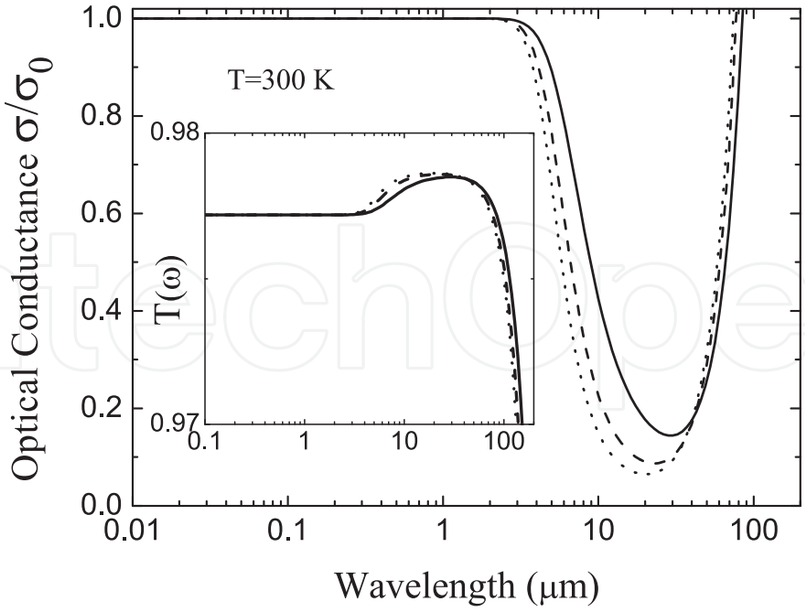

Fig. 7. Optical conductance and transmission coefficient (inset) as a function of the radiation wavelength, at room temperature, for different dark electron densities $n_0 = 5 \times 10^{11}$ cm^{-2} (solid curve), 8×10^{11} cm^{-2} (dashed curve), and 1×10^{12} cm^{-2} (dotted curve).

infrared bandwidth that was observed experimentally (Kuzmenko et al., 2008; Nair et al., 2008).

The optical conductance σ and transmission coefficient $T(\omega)$ are shown in Fig. 7 as a function of the radiation wavelength at room-temperature for different dark electron densities n_0. We note that the Fermi level for electrons becomes higher with increasing dark electron density. A higher Fermi level for electrons implies that the empty states in the conduction band have higher energies because of the linear shape of the energy spectrum for graphene. Since the optical transitions occur mainly via exciting electrons from occupied states to the empty states, a higher Fermi level corresponds to a higher transition energy. Thus, a blue shift of the optical absorption window can be observed in graphene samples with larger dark electron densities as shown in Fig. 7. This blue shift, with increasing gate voltage, has been observed experimentally (Li et al., 2008). Because in graphene the dark electron density increases almost linearly with increasing gate voltage (Novoselov et al., 2005), the theoretical results shown in Fig. 7 are in agreement with these experimental findings obtained from optical absorption measurements (Li et al., 2008). Furthermore, we find that the height of the absorption window increases with dark electron density and a sharper cut-off of the optical absorption at the window edges can be observed for larger electron densities. These theoretical results suggest that the width and height of the infrared absorption window in graphene can be controlled by applying a gate voltage. This feature can be utilized for making graphene-based and frequency-tunable infrared optoelectronic devices.

4. Conclusions

In this study we have examined theoretically the effect of optical phonon scattering on the optoelectronic properties of graphene. On the basis of the Boltzmann equation approach, we have derived the mass-balance and energy-balance equations for graphene in the presence

of a linearly polarized radiation field and of the electron-photon-phonon coupling. By solving these equations self-consistently, we have been able to determine the photo-excited carrier densities and optoelectronic coefficients, such as the optical conductance and light transmittance, for an air-graphene-wafer system. In particular, we have investigated the dependence of the photo-induced carrier densities, optical conductance, and transmission coefficient on intensity and wavelength of the radiation field, along with those on temperature and dark electron density. The main conclusions we have obtained are summarized as follows.
Because graphene is a gapless electronic system, electron-phonon interaction is an important mechanism in affecting the electronic transitions via both intra- and inter-band transition channels. In graphene the electrons in the valence band can gain the energy from the radiation field via optical absorption and be excited into the conduction band. At the same time, the electrons in the conduction band can lose energy via emission of phonons and be relaxed into the valence band. Thus, electron-phonon scattering can affect strongly the inter-band transition in contrast to conventional semiconductors. As a result, the electron-photon-phonon interaction is a major scattering mechanism to determine photo-induced carrier densities and optoelectronic properties of graphene.
In the presence of a radiation field, the photo-excited carrier densities in graphene first increase and then decrease with increasing radiation wavelength. The largest carrier densities caused by light radiation can be observed when the radiation photon energy equals to the optical phonon energy of graphene. Such resonant transitions are electrically equivalent to the electro-phonon resonance effect observed in conventional two-dimensional electron gas systems. The photo-excited carrier densities depend strongly on the radiation intensity and frequency, temperature, and dark carrier density.
In the short-wavelength regime ($\mathcal{L} < 3\ \mu$m), the universal optical conductance $\sigma_0 = e^2/(4\hbar)$ and light transmittance $T_0 \sim 0.98$ can be achieved for an air-graphene-SiO_2/wafer system. The optical conductance and transmission coefficient depend very little on temperature and dark electron density. These results agree with other theoretical works and with experimental findings.
We have found that there is an optical absorption window in the radiation wavelength range $4 \sim 100\ \mu$m. This infrared absorption window is induced by different transition energies required for inter- and intra-band optical absorption in the presence of the Pauli blockade effect. The depth and width of such an absorption window depend sensitively on the temperature and dark electron density in the sample due to the presence of a free-carrier absorption in this radiation wavelength regime. A prominent cut-off of the optical absorption can be observed at the edges of the window at lower temperatures and/or larger dark electron densities. These results can explain why experimentally the optical absorption window can be measured under long-wavelength radiation and why experimentally a blue shift of such a window can be observed when increasing the gate voltage.
The results obtained from this study indicate that in addition to the excellent optical properties of graphene in the visible regime, i.e., universal optical conductance, high light transmittance, etc., graphene can exhibit interesting and important features in the mid-infrared bandwidth, such as the optical absorption window. The width and the depth of this window can be tuned by varying the dark carrier density via, e.g., applying a gate voltage. This implies that graphene can be used as a frequency-tunable optoelectronic device operating in the mid-infrared bandwidth at room temperature for various applications. Together with the relevant phenomena discovered by very recent experimental work (Kuzmenko et al., 2008; Li et al., 2008; Choi et al., 2009), we hope that the present work sheds some light on the

application of graphene not only as a visible optoelectronic device but also as an infrared device in ambient conditions.

5. References

Novoselov, K.S.; Geim, A.K.; Morozov, S.V.; Jiang, D.; Zhang, Y.; Dubonos, S.V.; Grigoreva, I.V. & Firsov, A.A. (2004). Electric Field Effect in Atomically Thin Carbon Films, *Science* 306, pp. 666-669.

Zhang, Y.B.; Tan, Y.W.; Stormer, H.L.; & Kim, P. (2005). Experimental observation of the quantum Hall effect and Berry's phase in graphene, *Nature (London)* 438, pp. 201-204.

Berger C.; Song, Z.M.; Li, X.b.; Wu, X.S.; Brown, N.; Naud, C.; Mayou, D.; Li, T.B.; Hass, J.; Marchenkov, A.N.; Conrad, E. H.; First, P. N. & Heer, Walt A. de (2006). Electronic Confinement and Coherence in Patterned Epitaxial Graphene, *Science* 312, PP. 1191-1196.

Novoselov, K.S.; Geim, A.K.; Morozov, S.V.; Jiang, D.; Katsnelson, M.I.; Grigorieva, I.V.; Dubonos, S.V. & Firsov, A.A. (2005). Two-dimensional gas of massless Dirac fermions in graphene, *Nature* 438, PP. 197-200.

Castro, E. V.; Novoselov, K.S.; Morozov, S.V.; Peres, N.M.R.; Lopes dos Santos, J.M.B.; Nilsson, J.; Guinea, F.; Geim, A.K. & Castro Neto, A.H. (2007). Biased Bilayer Graphene: Semiconductor with a Gap Tunable by the Electric Field Effect, *Phys. Rev. Lett.* 99, PP. 216802-216805.

González, J. & Perfetto, E. (2008). Critical currents in graphene Josephson junctions, *J. Phys.: Condens. Matter* 20, pp. 145218-145226.

Lin, Y.M.; Jenkins, K. A.; Alberto V.G.; Small, J. P.; Farmer, D.B. & Avouris, P. (2009). Operation of Graphene Transistors at Gigahertz Frequencies, *Nano Letters* 9, pp. 422-426.

Eda, G.; Fanchini, G.; & Chhowalla, M. (2008). Large-area ultrathin films of reduced graphene oxide as a transparent and flexible electronic material, *Nature Nanotechnol.* 3, pp. 270-274.

Hogan, Hank (2008). *Photonics Spectra* 42, pp. 19.

Kuzmenko, A.B.; Heumen, E. van; Carbone, F.; & Marel, D. van der (2008). Universal Optical Conductance of Graphite, *Phys. Rev. Lett.* 100, pp. 117401-117404.

Li, Z.Q.; Henriksen, E.A.; Jiang, Z.; Hao, Z.; Martin, M.C.; Kim, P.; Stormer, H.L.; & Basov, D.N. (2008). Dirac charge dynamics in graphene by infrared spectroscopy, *Nat. Phys.* 4, pp. 532-535.

Nair, R.R.; Blake, P.; Grigorenko, A.N.; Novoselov, K.S.; Booth, T.J.; Stauber, T.; Peres, N.M.R. & Geim, A.K. (2008). Fine Structure Constant Defines Visual Transparency of Graphene, *Science* 320, pp. 1308.

Choi, H.; Borondics, F.; Siegel, D.A.; Zhou, S.Y.; Martin, M.C.; Lanzara, A. & Kaindl, R.A. (2009). Broadband electromagnetic response and ultrafast dynamics of few-layer epitaxial graphene, *Appl. Phys. Lett.* 94, pp. 172102-172104.

Wang, F.; Zhang, Yuanbo; Tian, Chuanshan; Giri, Caglar; Zettl, Alex; Crommie, Michael & Shen, Y. Ron (2008). Gate-Variable Optical Transitions in Graphene, *Science* 320, pp. 206-209.

Vasko, F.T. & Ryzhii, V. (2008). Photoconductivity of intrinsic graphene, *Phys. Rev. B* 77, pp. 195433-195440.

Falkovsky, L.A. & Pershoguba, S.S. (2007). Optical far-infrared properties of a graphene monolayer and multilayer, *Phys. Rev. B* 76, pp. 153410-153413.

Stauber, T.; Peres, N.M.R. & Geim, A.K. (2008). Optical conductivity of graphene in the visible region of the spectrum, *Phys. Rev. B* 78, pp. 085432-085439.

Ando, T. (2007). Magnetic Oscillation of Optical Phonon in Graphene, *J. Phys. Soc. Jpn.* 76, pp. 024712-024729.

McCann, E. & Falko, V.I. (2006). Landau-Level Degeneracy and Quantum Hall Effect in a Graphite Bilayer, *Phys. Rev. Lett.* 96, pp. 086805-086808.

Stroscio. Michael A. & Mitra Dutta (2005). *Phonons in Nanostructures*, Cambridge University Press, Cambridge.

Xu, W.; Peeters, F.M. & Lu, T.C. (2009). Dependence of resistivity on electron density and temperature in graphene, *Phys. Rev. B* 79, pp. 073403-073406.

Tse, Wang-Kong & Sarma S. Das (2007). Phonon-Induced Many- Body Renormalization of the Electronic Properties of Graphene, *Phys. Rev. Lett.* 99, pp. 236802-236805.

See, e.g., Xu, W.; Peeters, F.M.; & Devreese, J.T. (1991). Diffusion-to-streaming transition in a two-dimensional electron system in a polar semiconductor, *Phys. Rev. B* 43, pp. 14134-14141.

See, e.g., Xu, W. (2005). Screening length and quantum and transport mobilities of a heterojunction in the presence of the Rashba effect, *Phys. Rev. B* 71, pp. 245304-245312.

See, e.g., Lei, X.L. (1998). Balance-equation approach to hot- electron transport in semiconductors irradiated by an intense terahertz field, *J. Appl. Phys.* 84, pp. 1396-1404.

Dong, H.M.; Xu, W.; Zeng, Z.; Lu, T.C. & Peeters, F.M. (2008). Quantum and transport conductivities in monolayer graphene, *Phys. Rev. B 77*, pp. 235402-235410.

Wei, X.F.; Xu, W & Zeng, Z. (2007). Two-colour mid- infrared absorption in an InAs/GaSb-based type II and broken-gap quantum well, *J. Phys.: Condens. Matter* 19, pp. 506209-506215.

Sun, Dong; Wu, Zong-Kwei; Divin, Charles; Li, Xuebin; Berger, Claire; de Heer, Walt A.; First, Phillip N. & Norris, Theodore B. (2008). Ultrafast Relaxation of Excited Dirac Fermions in Epitaxial Graphene Using Optical Differential Transmission Spectroscopy, *Phys. Rev. Lett.* 101, pp. 157402-157405.

Xu, W.; Peeters, F.M. & Devreese, J.T. (1993). Electrophonon resonances in a quasi-two-dimensional electron system, *Phys. Rev. B* 48, pp. 1562-1570.

See, e.g., Li, Sheng S. (2006). *Semiconductor Physical Electronics* (2nd Edition) (Springer-Verlag, Berlin).

Krenner, H.J.; Clark, E.C.; Nakaoka, T.; Bichler, M.; Scheurer, C.; Abstreiter, G. & Finles, J.J.(2006). Optically Probing Spin and Charge Interactions in a Tunable Artificial Molecule, *Phys. Rev. Lett.* 97, pp. 076403-076406.

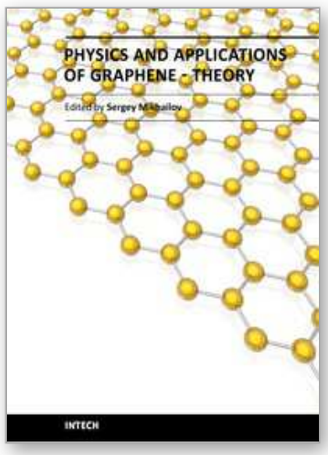

Physics and Applications of Graphene - Theory

Edited by Dr. Sergey Mikhailov

ISBN 978-953-307-152-7
Hard cover, 534 pages
Publisher InTech
Published online 22, March, 2011
Published in print edition March, 2011

The Stone Age, the Bronze Age, the Iron Age... Every global epoch in the history of the mankind is characterized by materials used in it. In 2004 a new era in material science was opened: the era of graphene or, more generally, of two-dimensional materials. Graphene is the strongest and the most stretchable known material, it has the record thermal conductivity and the very high mobility of charge carriers. It demonstrates many interesting fundamental physical effects and promises a lot of applications, among which are conductive ink, terahertz transistors, ultrafast photodetectors and bendable touch screens. In 2010 Andre Geim and Konstantin Novoselov were awarded the Nobel Prize in Physics "for groundbreaking experiments regarding the two-dimensional material graphene". The two volumes Physics and Applications of Graphene - Experiments and Physics and Applications of Graphene - Theory contain a collection of research articles reporting on different aspects of experimental and theoretical studies of this new material.

How to reference

In order to correctly reference this scholarly work, feel free to copy and paste the following:

W. Xu and H.M. Dong (2011). Photo-Induced Carrier Density, Optical Conductance and Transmittance in Graphene in the Presence of Optic-Phonon Scattering, Physics and Applications of Graphene - Theory, Dr. Sergey Mikhailov (Ed.), ISBN: 978-953-307-152-7, InTech, Available from: http://www.intechopen.com/books/physics-and-applications-of-graphene-theory/photo-induced-carrier-density-optical-conductance-and-transmittance-in-graphene-in-the-presence-of-o

INTECH
open science | open minds

InTech Europe
University Campus STeP Ri
Slavka Krautzeka 83/A
51000 Rijeka, Croatia
Phone: +385 (51) 770 447
Fax: +385 (51) 686 166
www.intechopen.com

InTech China
Unit 405, Office Block, Hotel Equatorial Shanghai
No.65, Yan An Road (West), Shanghai, 200040, China
中国上海市延安西路65号上海国际贵都大饭店办公楼405单元
Phone: +86-21-62489820
Fax: +86-21-62489821

IntechOpen